ChemComm

COMMUNICATION

View Article Online
View Journal | View Issue

Cite this: *Chem. Commun.*, 2015, **51**, 6601

Received 30th January 2015,
Accepted 10th March 2015

DOI: 10.1039/c5cc00885a

www.rsc.org/chemcomm

A continuous-flow mass biosensor for the real-time dynamic analysis of protease inhibition†

Yanyan Huang, Qundan Zhang, Guoquan Liu and Rui Zhao*

A flow injection analysis–quartz crystal microbalance (FIA–QCM) biosensor was developed for probing the dynamic interactions during protease inhibition. Being sensitive to conformation features of different proteases, this continuous-flow sensor has potential for structural–functional analysis and inhibitor selection.

Proteases are responsible for various physiological processes, including metabolism, cell signalling and immune response.[1,2] To maintain their functions, protease inhibition, which turns off the catalytic activity, plays a key role in the regulation mechanism.[3] To better understand the structural–functional relationships of proteases, real-time, selective and sensitive analysis of dynamic interactions during inhibition is essential.

Thus far, some methods have been developed for analyzing enzyme activity and inhibition kinetics. The stopped-flow approach, as a conventional way to measure enzymatic activity in bulk solutions, has been applied for kinetic study of proteases.[4] With high sensitivity, fluorescence/colorimetric sensors have been designed for monitoring protease activity and inhibitor screening.[5–7] Smart micro/nanomaterials have also been employed for studying enzymatic reactions and protease inhibition.[8] Nevertheless, these specially tailored materials and devices are skilfully designed or commercially unavailable. More importantly, specific and multi-step labelling techniques are usually required for signal processing. And real-time analysis of the inhibition kinetics in terms of specific conformations is still limited.

Quartz crystal microbalance (QCM), as a simple, sensitive and label-free mass sensor, has been successfully applied in the fields of materials science,[9] biophysics,[10] organic reactions[11] and bioanalysis.[12] Due to the advantage of its unique label-free and real-time nature, QCM is becoming a powerful tool for direct monitoring of biomolecular interactions.[13] For enzymatic reactions, efforts have been devoted to the investigation of DNA polymerization/cleavage, telomerase activity change and protein degradation.[14] The emergence of the flow injection analysis (FIA) technique opens a new opportunity for QCM study of a protease reaction in a continuous flow mode, which has the advantage of supplying the crystal interface with always-fresh analytes and thus may better mimic the enzymatic process *in vivo*.

In this study, an FIA–QCM biosensing system was utilized for the on-line analysis of protease inhibition. This FIA–QCM system is promising for the rapid and efficient analysis of dynamic interactions between enzymes, substrates and inhibitors, especially with respect to the structure-sensitive inhibition kinetics. By immobilizing a trypsin inhibitor (abbreviated as TI, from soybean, type I-S, 20.1 kDa) as a specific ligand, the kinetic interaction between TI and two serine proteases (trypsin and chymotrypsin), and an aspartate protease pepsin was investigated in real-time (Scheme 1). The software based on a genetic algorithm[15] was used to analyze the kinetic processes of inhibition. With the attempt to understand the structural–functional relationships, further investigation into the protein conformations during the kinetic inhibition of proteases was carried out.

The preparation procedure of the QCM sensor is illustrated in Scheme 1. A gold surface was firstly functionalized

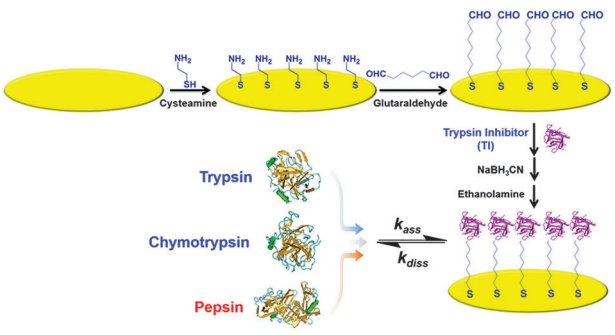

Scheme 1 Schematic illustration of the preparation of the TI-immobilized quartz crystal surface and its application for the dynamic analysis of protease binding.

Beijing National Laboratory for Molecular Sciences, CAS Key Laboratory of Analytical Chemistry for Living Biosystems, Institute of Chemistry, Chinese Academy of Sciences, Beijing 100190, China. E-mail: zhaorui@iccas.ac.cn; Fax: +86-10-62559373; Tel: +86-10-62557910

† Electronic Supplementary Information (ESI) available. See DOI: 10.1039/c5cc00885a

by a self-assembling monolayer of cysteamine through Au–S bonds. To provide TI with flexible spatial orientation, different bi-functional linker molecules were examined. Glutaraldehyde was employed as an optimal spacer to react with the amino groups of cysteamine and TI (ESI†). The changes in frequency were monitored during the modification process. After immobilizing TI, the decrease in frequency was 91 Hz. According to the Sauerbrey equation,[16] the density of TI on the gold surface was calculated to be 400 ng cm^{-2} (20 pmol cm^{-2}), which is sufficient for studying the molecular interaction and obtaining free binding conformation and flexibility for the immobilized TI.[17]

Since the three-dimensional structures and inhibitory binding of proteases are pH dependent,[18] the optimum pH condition for protease–inhibitor interaction was investigated using the FIA–QCM system. For trypsin, the change in frequency increased as the pH rose from 5.5 to 7.5 and reached a plateau between pH 7.5 and 8.5 (Fig. 1a). This is well consistent with the fact that the strongest inhibition activity of TI is observed at around 8.0.[19] For chymotrypsin, a similar response profile was detected with the largest change in frequency being at pH 7.5. Differently, an obvious decrease in frequency response was observed at pH 8.5. This may be attributed to the loss in electrostatic interaction of chymotrypsin towards TI, because chymotrypsin almost became charge-balanced at pH 8.5, which is close to its isoelectric point (pI 8.75). As the control protease, pepsin induced a much lower signal change in the pH range. Hence, pH 7.5 was selected as the optimized pH for studying the dynamic interactions between TI and proteases. Also, the glycine–HCl buffer with good elution efficiency was chosen for surface regeneration (Fig. S1, ESI†). After 30 rounds of the binding–dissociation process, the loss of the signal was only 3.3% at the 30th injection, suggesting good stability and reproducibility of the sensor (Fig. S2, ESI†).

For investigating the enzyme–inhibitor interaction, sensing curves obtained by the injection of different proteases were recorded as shown in Fig. 1b. Significant frequency decreases of 53.9 ± 2.09 Hz and 55.8 ± 2.33 Hz (n = 3) occurred for trypsin and chymotrypsin respectively. Such a significant binding of these two proteases is in accordance with the fact that TI as a typical Kunitz trypsin inhibitor specially binds serine proteases, such as trypsin and chymotrypsin.[20] In comparison, pepsin, as an aspartate protease, only causes a frequency change of 24.7 ± 1.44 Hz (n = 3), suggesting a much weaker interaction. Moreover, a non-protease protein BSA was also examined, and no frequency response was detected even when the concentration of BSA was ten times higher (Fig. 1b).

To further demonstrate the selectivity of the sensor, QCM assays of trypsin, chymotrypsin and pepsin in the mixtures of different proteins were carried out. As shown in Fig. 2a, although coexisting with inference proteins including BSA, ribonuclease A, cytochrome c and lysozyme, trypsin and chymotrypsin can still cause decreases in frequency similar to those from individual injection assays. However, the coexistence of pepsin with other proteins only induced a frequency change of 9 Hz, which was significantly smaller than that obtained from individual measurements. This result suggests that the weak interaction between pepsin and TI can be easily interfered from other proteins. Thus it is clear that the QCM sensor enables the discrimination of trypsin and chymotrypsin even when they were coexisting with interference proteins.

Benefiting from the high specificity of the QCM sensor, proportional frequency responses to different concentrations of trypsin and chymotrypsin were achieved (Fig. S3, ESI†), suggesting the capability of the sensor for the quantitative determination of these serine proteases. The linear range for trypsin quantitation is 0.025 mg mL^{-1} to 0.125 mg mL^{-1}, and for chymotrypsin is 0.025 mg mL^{-1} to 0.10 mg mL^{-1}. From the calibration curves (Fig. 2b), the detection limits were found to be 3.8×10^{-3} mg mL^{-1} and 5.4×10^{-3} mg mL^{-1} for trypsin and chymotrypsin, respectively (signal/noise = 3 : 1), which are lower than those of some previously reported assays.[21]

In order to understand the kinetic nature of the interaction between TI and proteases, the entire binding and dissociation processes were analysed using the software based on a genetic algorithm and eqn S(1)–S(4), ESI.† Kinetic constants (k_{ass} and k_{diss}) and the equilibrium binding constants (K_A) were conveniently calculated (Table 1). It can be observed that chymotrypsin showed the fastest binding rate (8.45×10^2 L mol^{-1} s^{-1}), and trypsin revealed the slowest dissociation from TI (2.60×10^{-4} L s^{-1}). These results suggest the ease with which the chymotrypsin–TI complex can be formed. And the tight trypsin–TI complex led to the hindrance for disassembly. Considering both association and dissociation kinetics, the association constant of trypsin (2.30×10^6 L mol^{-1}) is larger than that for chymotrypsin

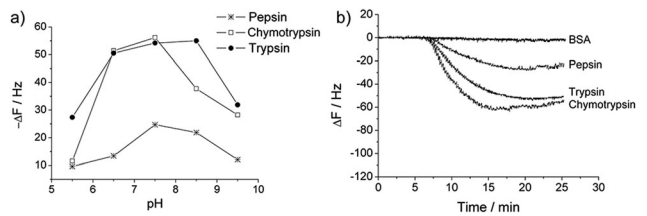

Fig. 1 (a) Effect of pH on the binding between TI and proteases. (b) Binding processes of the three proteases toward the immobilized TI on the QCM sensor. QCM sensing conditions: 25 °C, mobile phase: phosphate buffer (pH 7.5), BSA concentration: 1 mg mL^{-1}, and proteases concentration: 0.10 mg mL^{-1}.

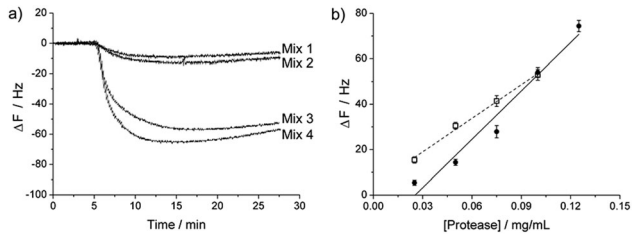

Fig. 2 (a) Selective sensing of trypsin and chymotrypsin in protein mixtures. Mixture 1 contains BSA, ribonuclease A, cytochrome c and lysozyme; mixtures 2, 3 and 4 are mixture 1 spiked with pepsin, trypsin and chymotrypsin, respectively. QCM sensing conditions: 25 °C, phosphate buffer (pH 7.5), concentration for each protein: 0.1 mg mL^{-1}. (b) Calibration curves of trypsin and chymotrypsin on the TI-immobilized biosensor (n = 3).

Table 1 Results of kinetic analysis for the interactions between the immobilized TI and three proteases

Enzyme	k_{ass} (L mol^{-1} s^{-1})	k_{diss} (L s^{-1})	K_A (L mol^{-1})	K_D (mol L^{-1})
Trypsin	6.02×10^2	2.60×10^{-4}	2.30×10^6	4.32×10^{-7}
Chymotrypsin	8.45×10^2	5.56×10^{-4}	1.57×10^6	6.58×10^{-7}
Pepsin	5.34×10^2	1.24×10^{-3}	4.30×10^5	2.32×10^{-6}

(1.57×10^6 L mol^{-1}). This agrees well with the fact that the Kunitz trypsin inhibitor can effectively inhibit trypsin, and to a lesser extent chymotrypsin.[22] In contrast, the slow association and fast dissociation of pepsin with TI accounts for the weak interaction between them.

Based on the above kinetic analysis, further investigation on the specific binding between TI and the three proteases was performed with regard to protease conformation. As the typical members of the serine protease family, both trypsin and chymotrypsin contain the characteristic Asp–His–Ser catalytic triad. Their specificity is usually rationalized by the topology of the binding sites and controlled by a small set of structural elements adjacent to the catalytic triad.[1] As illustrated in Fig. 3a and b, trypsin and chymotrypsin have a similar spatial structure and an active binding site S1.[23] The S1 site is a pocket formed by residues 189–192, 214–216 and 224–228. The difference in the S1 structures can account for the different inhibitory kinetics of TI towards two serine proteases. For chymotrypsin, Ser189, Gly216 and Gly226 create a hydrophobic pocket where hydrophobicity is the main driving force for specificity. In contrast, trypsin has Asp189, Gly216 and Gly226 forming a negatively charged pocket where electrostatic interaction is critical for the specific binding, and hydrophobic interaction is an additional force. The combination of electrostatic and hydrophobic interactions results in the stronger affinity of trypsin–TI (K_A 2.30×10^6 L mol^{-1}) than chymotrypsin–TI (K_A 1.57×10^6 L mol^{-1}).

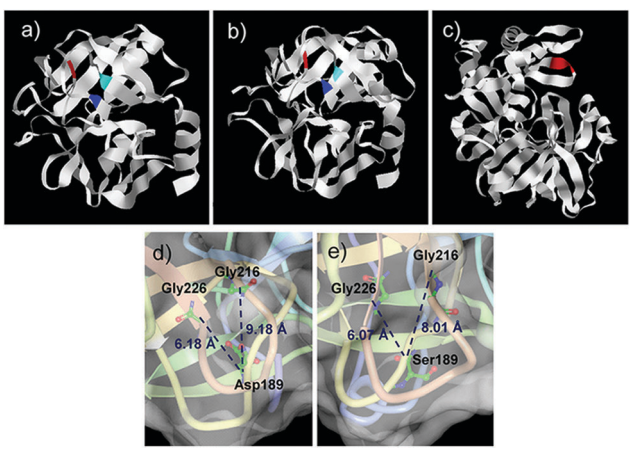

Fig. 3 Structural analysis of the three proteases. In trypsin (a) and chymotrypsin (b), Asp189 and Ser189 are shown in red, Gly216 is in blue, Gly226 is in cyan, and in pepsin (c), Asp–Ser–Cys sequence (280–282) is shown in red; (d, e) Structures of S1 pockets in trypsin (d) and chymotrypsin (e). Ribbon drawing of the three proteases were generated and analyzed with RASTOP software (a–c), and S1 structures with surfaces were generated by RSCB-Protein Workshop[25] (d, e).

It is also interesting that the fast association–dissociation kinetics of chymotrypsin–TI and the slow association–dissociation rate of the trypsin–TI complex can reflect different S1 structures. In both trypsin and chymotrypsin, Gly216 and Gly226 are located at the entrance of S1 sites with the function of selectively blocking the access of large substrates or inhibitors into the pockets. However, at the bottom of the pockets, trypsin has an Asp189 residue while chymotrypsin has Ser189 (Fig. 3).[24] From the protein crystal structures, the depth of S1 pockets can be measured by the distance between the two Gly residues and the position of 189 residues. For trypsin, the distance between Gly216 and Asp189 is 9.18 Å and the distance between Gly226 and Asp189 is 6.18 Å (Fig. 3d). In comparison, for chymotrypsin the distance between Gly216 and Ser189 is 8.01 Å and the distance between Gly226 and Asp189 is 6.07 Å (Fig. 3e). Obviously, the deeper S1 pocket of trypsin causes more difficulty to the TI to penetrate into the S1 site, which leads to slow association and dissociation processes. Such particular structural features make TI a more selective inhibitor for trypsin.

Pepsin was stable and retained its natural conformation under sensing conditions of pH 7.5 (ESI†). It was due to the lack of key structural elements such as the S1 pocket that pepsin could not be inhibited by TI.[26] However, a weak interaction between pepsin and TI was detected (Table 1). From kinetic data, this phenomenon can be ascribed to the presence of an Asp–Ser–Cys sequence in pepsin (residues 280–282, Fig. 3c), which is the same as the sequence at the bottom of the S1 site in trypsin (residues 189–191). The same sequence was also found at the S1 site of chymotrypsin (Ser–Ser) and in pepsin (ESI†). These similarities may lead to the non-specific binding between pepsin and TI. In contrast, these similar elements in pepsin are all located on the protein surface, thus leading to rapid dissociation behavior of pepsin–TI. The QCM results well reflect the different structural location of these sequences as well as the conformational features of pepsin and serine proteases.

The binding kinetics between TI and the three proteases trypsin, chymotrypsin and pepsin was analyzed using an FIA–QCM biosensor. This biosensor revealed high affinity and selectivity towards trypsin and chymotrypsin. Its real-time, label-free and sensitive nature enables the mass sensor to be responsive to the conformation features of these proteases with different interaction kinetics. Such dynamic sensing was facilely determined, indicating the great potential of the QCM biosensor in the structure analysis of proteases and for its applicability to the design and selection of novel inhibitors.

Financial support from the National Natural Science Foundation of China (21375134, 21135006, 21321003 and 21475140) and the Ministry of Science and Technology of China (2015CB856303) is acknowledged.

Notes and references

1 L. Hedstrom, *Chem. Rev.*, 2002, **102**, 4501.
2 N. G. Dandachi and S. D. Shapiro, *Nat. Med.*, 2014, **20**, 470.
3 (*a*) J. Van Griensven, E. Diro, R. Lopez-Velez, M. Boelaert, L. Lynen, E. Zijlstra, J.-C. Dujardin and A. Hailu, *Lancet Infect. Dis.*, 2013, **13**, 251; (*b*) A. R. Kennedy and X. S. Wan, *Prostate*, 2002, **50**, 125;

(*c*) R. Smoum, A. Rubinstein, V. M. Dembitsky and M. Srebnik, *Chem. Rev.*, 2012, **112**, 4156.
4 J. M. Zhou, C. Lin and C. L. Tsou, *Biochemistry*, 1989, **28**, 1070.
5 (*a*) P. Biswas, L. N. Cella, S. H. Kang, A. Mulchandani, M. V. Yates and W. Chen, *Chem. Commun.*, 2011, **47**, 5259; (*b*) Y. Huang, S. Xiong, G. Liu and R. Zhao, *Chem. Commun.*, 2011, **47**, 8319.
6 Y. Wang, Y. Zhang and B. Liu, *Anal. Chem.*, 2010, **82**, 8604.
7 Q. Zhang, W. Li, J. Chen, F. Wang, Y. Wang, Y. Chen and C. Yu, *Chem. Commun.*, 2013, **49**, 3137.
8 (*a*) C. Wang, J. Ouyang, Y. Y. Wang, D. K. Ye and X. H. Xia, *Anal. Chem.*, 2014, **86**, 3216; (*b*) X. Liu, Y. Li, X. Xu, P. Li, Z. Nie, Y. Huang and S. Yao, *TrAC, Trends Anal. Chem.*, 2014, **58**, 40.
9 J. John, K. M. Hugar, J. Rivera-Meléndez, H. A. Kostalik, IV, E. D. Rus, H. Wang, G. W. Coates and H. D. Abruña, *J. Am. Chem. Soc.*, 2014, **136**, 5309.
10 A. Webster, F. Vollmer and Y. Sato, *Nat. Commun.*, 2014, **5**, 5284.
11 M.-C. Tseng and Y.-H. Chu, *Anal. Chem.*, 2014, **86**, 1949.
12 (*a*) C. I. Cheng, Y.-P. Chang and Y.-H. Chu, *Chem. Soc. Rev.*, 2012, **41**, 1947; (*b*) Y. Shang, P. R. Singh, M. M. Chisti, R. Mernaugh and X. Zeng, *Anal. Chem.*, 2011, **83**, 8928; (*c*) B. Huang, N. Jia, L. Chen, L. Tan and S. Yao, *Anal. Chem.*, 2014, **86**, 6940; (*d*) P. He, L. Liu, W. Qiao and S. Zhang, *Chem. Commun.*, 2014, **50**, 1481; (*e*) Q. D. Zhang, Y. Y. Huang, R. Zhao, G. Q. Liu and Y. Chen, *Biosens. Bioelectron.*, 2008, **24**, 48.
13 (*a*) X. Xu, J. Zhou, X. Liu, Z. Nie, M. Qing, M. Guo and S. Yao, *Anal. Chem.*, 2012, **84**, 4746; (*b*) D. Z. Wang, W. Tang, X. J. Wu, X. Y. Wang, G. J. Chen, Q. Chen, N. Li and F. Liu, *Anal. Chem.*, 2012, **84**, 7008; (*c*) H. Furusawa, Y. Tsuyuki, S. Takahashi and Y. Okahata, *Anal. Chem.*, 2014, **86**, 5406.
14 (*a*) M. Lazerges, H. Perrot, N. Rabehagasoa, E. Antoine and C. Compere, *Chem. Commun.*, 2005, 6020; (*b*) H. Nishino, A. Murakawa, T. Mori and Y. Okahata, *J. Am. Chem. Soc.*, 2004, **126**, 14752; (*c*) H. Matsuno, H. Furusawa and Y. Okahata, *Chem. Commun.*, 2002, 470; (*d*) Y. Zhou, P. Zhou, Y. Xin, J. Wang, Z. Zhu, J. Hu, S. Wei and H. Ma, *Sci. Rep.*, 2014, **4**, 6978.
15 (*a*) Y. Liu, X. Yu, R. Zhao, D. H. Shangguan, Z. Y. Bo and G. Q. Liu, *Biosens. Bioelectron.*, 2003, **19**, 9; (*b*) A. Brunetti, *Comput. Phys. Commun.*, 2000, **124**, 204.
16 G. Sauerbrey, *Z. Phys.*, 1959, **155**, 206.
17 (*a*) S. M. Knudsen, J. Lee, A. D. Ellington and C. A. Savran, *J. Am. Chem. Soc.*, 2006, **128**, 15936; (*b*) K. Ohtsuka, R. Kajiki, M. Waki, T. Nojima and S. Takenaka, *Analyst*, 2004, **129**, 888.
18 M. Z. Atassi, C. J. van Oss and D. R. Absolom, *Molecular Immunology*, Marcel Dekker Press, New York, 1984.
19 W. R. Finkenstadt and M. Laskowski Jr., *J. Biol. Chem.*, 1965, **240**, 962.
20 M. Kunitz, *J. Gen. Physiol.*, 1946, 291.
21 (*a*) S. A. Grant, C. Weilbaecher and D. Lichlyter, *Sens. Actuators, B*, 2007, **121**, 482; (*b*) J.-P. Xu, Y. Fang, Z.-G. Song, J. Mei, L. Jia, A. J. Qin, J. Z. Sun, J. Ji and B. Z. Tang, *Analyst*, 2011, **136**, 2315; (*c*) V. D. Trivedi, B. Raman, T. Ramakrishna and Ch. M. Rao, *J. Biochem. Biophys. Methods*, 1999, **40**, 49.
22 U. De Vonis Bidlingmeyer, T. R. Leary and M. Laskowski, *Biochemistry*, 1972, **11**, 3303.
23 (*a*) D. Liebschner, M. Dauter, A. Brzuszkiewicz and Z. Dauter, *Acta Crystallogr., Sect. D: Biol. Crystallogr.*, 2013, **69**, 1447; (*b*) P. E. Pjura, A. M. Lenhoff, S. A. Leonard and A. G. Gittis, *J. Mol. Biol.*, 2000, **300**, 235; (*c*) L. Hedstrom, L. Szilagyi and W. J. Rutter, *Science*, 2007, **255**, 1249.
24 P. Chen, J. Rose, R. Love, C. H. Wei and B. C. Wang, *J. Biol. Chem.*, 1991, **267**, 1990.
25 (*a*) J. L. Moreland, A. Gramada, O. V. Buzko, Q. Zhang and P. E. Bourne, *BMC Bioinf.*, 2005, **6**, 21; (*b*) D. Xu and Y. Zhang, *PLoS One*, 2009, **4**, e8140.
26 B. M. Dunn, *Chem. Rev.*, 2002, **102**, 4431.

